

CN9000984

CNIC-00304

ASIPP-0009

# 中国核科技报告

CHINA NUCLEAR SCIENCE & TECHNOLOGY REPORT

用RHF在HT-6B托卡马克上研究等离子

体的约束和锯齿振荡行为

INVESTIGATION OF SAWTOOTH BEHAVIOR

AND CONFINEMENT PROPERTY WITH

RHF ON THE HT-6B TOKAMAK



原子能出版社

中国核情报中心

China Nuclear Information Centre

**CNIC-00304**

**ASIPP-0009**

**用RHF在HT-6B托卡马克上研究等离子  
体的约束和锯齿振荡行为**

**INVESTIGATION OF SAWTOOTH BEHAVIOR  
AND CONFINEMENT PROPERTY WITH  
RHF ON THE HT-6B TOKAMAK**

**霍裕平 谢纪康 李林忠 何也熙  
郭德全 秦品建 李国相 邓传宝  
黄 荣 郭其良 童兴德 赵君煜**

**(中国科学院等离子体物理研究所, 合肥)**

**中国核情报中心  
原子能出版社**

**北京·1989.1**

## 摘 要

给出了HT-6B托卡马克上的共振螺旋场(RHF)对等离子体的约束和锯齿振荡行为影响的实验结果。RHF使电子热导减小、电子温度分布变宽、等离子体密度增加并增强了杂质辐射,同时使锯齿振荡增强(包括锯齿幅度、周期、上升率及反相半径)和 $m=2,3,4$ 的MHD不稳定性被抑制。实验结果表明RHF使放电进入一个新的放电状态。

**关键词** 托卡马克装置 等离子体约束 锯齿振荡

# INVESTIGATION OF SAWTOOTH BEHAVIOR AND CONFINEMENT PROPERTY WITH RHF ON THE HT-6B TOKAMAK

Huo Yuping      Xie Jikang      Li Linzhong  
He Yexi          Guo Dequan      Qin Pinjian  
Li Guoxiang      Deng Chuanbao      Huang Rong  
Guo Qiliang      Tong Xingde      Zhao Junyu

(Institute of Plasma physics, Academia sinica, Hefei)

## ABSTRACT

The experiment results of The resonant helical field (RHF) effects on plasma confinement and sawtooth behavior on the HT-6B Tokamak are presented. The RHF makes decrease of electron thermal conductivity, broadening of temperature profile, increase of plasma density and enhancement of impurity radiation, at meanwhile intensification of sawtooth oscillation (in amplitude, period, rising slope and invert radius) and suppression of  $m=2, 3, 4$  modes. It is shown that the discharge transforms to a new discharge condition.

# 1. INTRODUCTION

Investigation of the external helical magnetic perturbation effect on MHD modes has been of extensive interests since the first result was obtained on the Pulsator tokamak. Experiment results on HT-6B that a weak resonant helical field (RHF) suppresses MHD modes ( $m=2, 3, 4, 5$ ) were reported in Ref. [1], [2], [3]. The suppression was explained by a resonant mechanism and a strong global correlation between different modes. It was observed that the RHF also affect sawtooth behavior. Recent experiment result showed that these effects are accompanied by the improvement of plasma confinement. That made the picture more complicated.

## 2. SAWTOOTH BEHAVIOR WITH THE RHF

On the HT-6B tokamak sawtooth behavior was influenced by RHF over a wide range of operation parameters, such as  $\bar{n}_e=(0.6\sim 3)\times 10^{11}\text{cm}^{-3}$ ,  $q=2.6\sim 5$ . The optimal amplitude and configuration ( $l=2$  or  $3$ ) of RHF depended on the operation conditions. Nevertheless RHF was always lower than 1% of poloidal field. Experiment results were given in two categories according to the plasma densities.

In the first case, at low density ( $\bar{n}_e < 1.5 \times 10^{11}\text{cm}^{-3}$ ), sawteeth in a normal discharge would be amplified by a pulsed DC RHF. Fig.1 (a) shows the signals of the soft X-ray diode array and  $m=3$  magnetic perturbation vs time. For comparison we also put the amplified sawteeth together with the former ones on an expanded time coordinate in Fig.1 (b).

When the RHF turned on, at 12 ms, sawteeth were amplified in amplitude, period and fluctuation slope. The fluctuation magnitudes increased by a factor of 2.5 up to about 1/3 of the mean value on soft X-ray signal of the central chord. The periods prolong from 230 $\mu\text{s}$  to 320 $\mu\text{s}$ . The ramp up slope increased from 0.9V/ms to 1.5V/ms and the collapse slope from 3.6V/ms to 7.6V/ms.

In the case of  $\bar{n}_e > 1.5 \times 10^{11}\text{cm}^{-3}$ , discharge normally had strong Mirnov oscillations. That magnetic perturbation was about 1% of the poloidal field. In Fig.2(a), soft X-ray signals of different radii and Mirnov probe signals were modulated by 24kHz oscillations. At 8 ms the RHF turning on, Mirnov oscillations transformed to sawteeth. These sawteeth had larger amplitudes than those in Fig.1. In some discharges the sawtooth fluctuation might spread over the plasma volume which could be observed on diode signal at 10cm, on hard X-ray signal (collimated to limiter) and mirnov probe signals.

Fig.2(b) and 2(c) show the time expanded curves round the moments where RHF was put on and off respectively. One can see with RHF on 24kHz oscillation decrease and sawteeth appear from center to edge and enlarge to a high saturated amplitude. The inverse process took place when RHF was turned off. The relax times of these two processes were near 1 ms, which was close to the energy confinement time ( $\tau_E \sim 0.7$  ms).

In both cases, the 24kHz Mirnov oscillations were identified as  $m=1$  mode at  $r < 4$ cm and  $m=2,3$  at  $r > 6$ cm region. The suppression of modes and occurrence of sawteeth kept the same pace. This was an argument about the driven force of the sawtooth collapse. It seemed that the suppressed small  $m=1$  mode could not be able to drive the intensive collapse at the plasma hot core.

### 3. PLASMA CONFINEMENT IMPROVEMENT BY RHF

Electron thermal conductivity was derived from calculation of the time decay between sawtooth collapses at different radii<sup>(4)</sup>. Result was given in table 1. With RHF effect  $X_e$  decreased to 3/4 in the core and to 2/3 in outer region. The reduction of  $X_e$  was in good agreement with the increment of sawtooth ramp up slope.

Electron temperature profile  $T_e(r)$  was derived from soft X-ray measurement. As was shown in Fig.3, the profile became broader.  $T_e$  in outer region ( $r > r_s$ ) increased and  $\bar{T}_e$  (average over sawteeth) at the centre became a bit lower. That cooling effect on plasma centre might attribute to the large sawtooth perturbations. Considering the fluctuation, the large sawteeth made  $T_e$  fluctuate to a higher maximum and a deeper minimum. In our experiments, line averaged electron density  $n_e$  showed a gradual increase with RHF proportional to time. For example,  $n_e$  arised up to  $1.6 \times 10^{17} \text{cm}^{-3}$  in 20 ms with RHF, comparing to  $1.1 \times 10^{17} \text{cm}^{-3}$  in a reference discharge without RHF, and with the same gas-puffing procedure.

Fig.4 gives the measurement results of line emissions. OIII(375.99nm), CIII(464.74nm) and H $\alpha$ (656.3nm) lines were monitored with a multi-fibre channel mono-spectrometer with 0.6cm space resolution. It could be seen that the line emissions of light impurities held a plateau during RHF was on from 8 ms to 14.2 ms. Its magnitude was about half of its original value. The rising and falling processes synchronized with the sawtooth transform processes shown in Fig.2 (b), 2(c). These plateau appeared on channels of the spectroscopic viewing chords over the whole plasma, even at 11cm radius. The phenomenon could not be easily explained. It should be sensitive to temperature and density rise and impurity accumulation. The rising and falling time is in the order of 1 ms. It

is too fast for explanation with neoclassical accumulation and diffusion of impurities. There need more accurate diagnostics and a careful calculation.

In Fig.4,  $H_\alpha$  radiation behaved different from impurities. It rised in first 2 ms and immediately decayed to its original value, without significant change when RHF turned off. That showed there was no much intensed Hydrogen influx during that period.

Table 1 Reduction of  $X_e$  at center and 7.6 cm by RHF

| shot 11176  | $X_e$ ( $m^2s^{-1}$ ) |                 |
|-------------|-----------------------|-----------------|
|             | $r=0cm$               | $r=7.6cm$       |
| without RHF | $3.38 \pm 0.49$       | $7.76 \pm 0.15$ |
| with RHF    | $2.37 \pm 0.38$       | $4.30 \pm 0.30$ |

The results mentioned above showed that the weak RHF magnetic perturbation would change the MHD instabilities, sawtooth behavior as well as plasma confinement. On opposite, the effectiveness of RHF depended on the plasma condition. RHF was not effective in high  $Z_{eff}$  discharge. RHF configuration ( $i=2$  or  $3$ ) had to be chosen for discharge: with different  $q$  values and profiles. The optimal RHF current was related to plasma density. It meant that the mechanism of RHF could not be simply considered as a direct magnetic interaction with MHD mode.

#### 4. SUMMARY

Main experiment results can be summarized as follows:

- (a) RHF could reduce energy and partical losses and improve plasma confinement. RHF discharges have higher density and broader temperature profile.
- (b) RHF produced large sawteeth characterized by their amplitudes, periods, slopes and the range where the sawteeth spread over. The large amplitude sawteeth with strong collapses decreased the mean value of temperature at the plasma core. It is unclear that why the driven force of the collapses were intensified and what kind the driven force is.
- (c) The line emissions of light impurities increased over the whole plasma. It showed a plateau during RHF on, which was different from the successive grow of  $\bar{n}_e$ .
- (d) The DC RHF could suppress the Mirnov oscillation, improve the confinement, but could also amplify the sawteeth and enhance impurity radiation... It is quite difficult to understand all of such phenomena from physical picture of usual tokamak discharge. It seems to be a new state of tokamak plasma.

## CAPTIONS

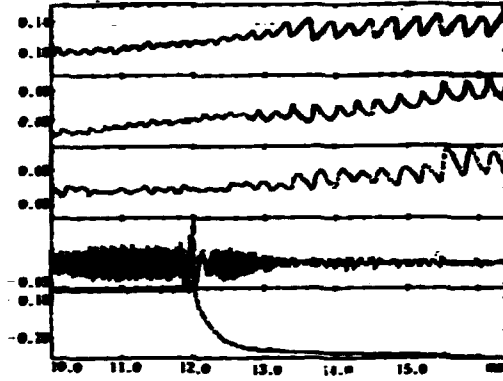


**Fig.1(a)** Sawteeth amplification by RHF from 12 ms, curves from the top are soft X-ray signals at 2, 6, 8 cm,  $m=3$  and helical current (inverted) respectively

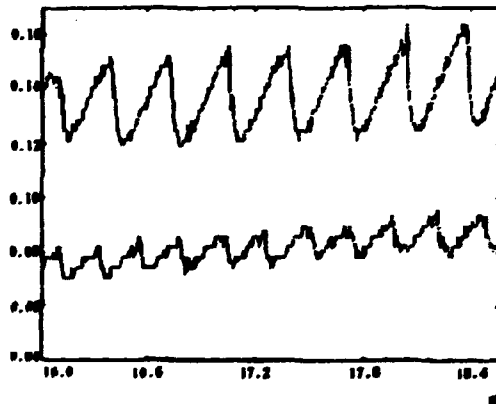


**Fig.1(b)** Sawteeth with (top curve) and without (bottom curve) RHF



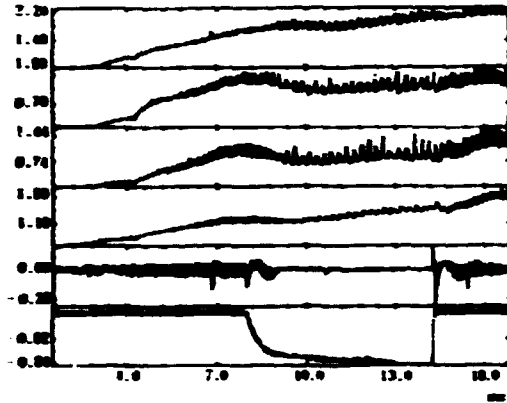


Fig.2(a) Discharge transformation from 24kHz oscillation to large sawteeth by RHF. Curves are soft X-ray signals at 2, 4, 6, 8 cm,  $m=3$ , RHF current (inverted)

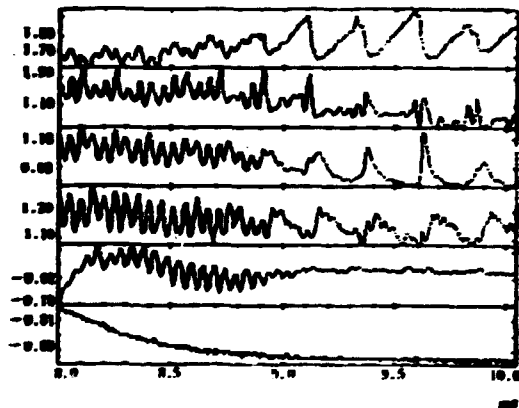


Fig.2(b) Signals with expanded time scale at moments of RHF on and off respectively

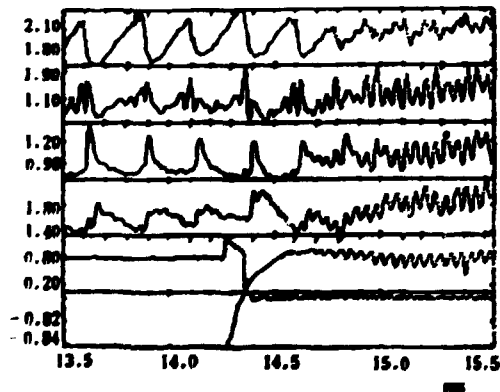


Fig.2(c) Signals with expanded time scale at moments of RHF on and off respectively

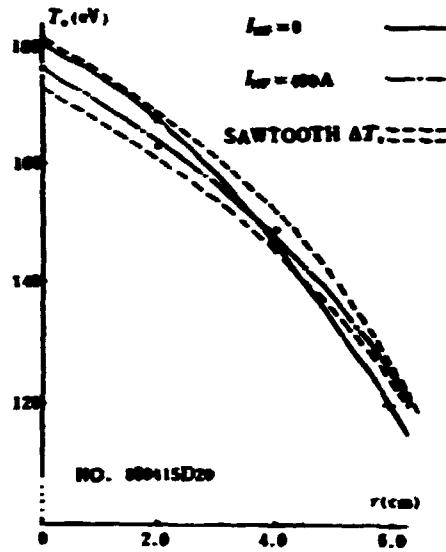


Fig.3  $T_e(r)$  derived from soft X-ray measurement broadening with RHF

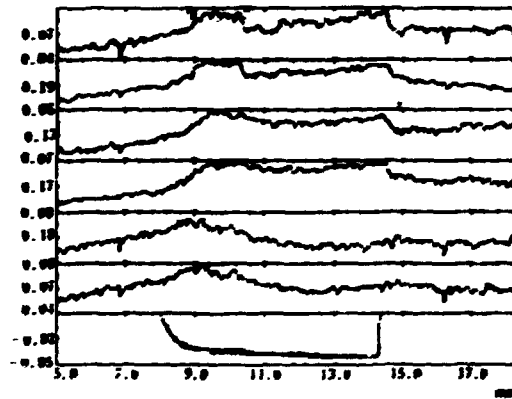


Fig.4 Line emission signals of OIII (at 1.5 cm and 8.7 cm), CIII (at 1.5 cm and 8.7 cm),  $H_\alpha$  (at 1.5 cm and 8.7 cm) and RHF current (inverted)

#### REFERENCES

- [1] ZHIAO Qingchu, et al., "Suppression of Tearing Modes in Tokamaks by a Helical Magnetic Field" (Proc. 10th Int. Conf. London, 1984), Vol.1, P.345
- [2] Xie Jikang, Chen Jiayu, Guo Wenkang, Huo Yuping, et al., "Studies of MHD MODES and High Frequency Fluctuations on the HT-6B and HT-6M Tokamaks", (Proc. 11th Int. Conf. Kyoto, 1986), Vol.1, P. 317
- [3] Xie Jikang, Huo Yuping, Chen Jiayu, et al., "Modification of Sawtooth Behavior Using RHF on HT-6B Tokamak", (Proc. 14th Euro. Conf. Madrid, 1987) Vol. 11D part 1, P.221
- [4] Collen, J. D., Jahns, G. L., Phys. Rev. Lett. Vol. 38, (1977) 401.

## 一、引言

自从人们在Pulsator托卡马克上最初获得外部螺旋场对等离子体MHD不稳定性的影响的初步结果以来,人们对这一研究课题一直有着浓厚的兴趣。在参考文献[1]、[2]和[3]中报告了HT-6B托卡马克上弱共振螺旋场(RHF)对等离子体中 $m=2,3,4,5$ 的MHD不稳定模式的抑制的实验结果。这种抑制作用被解释为一个共振机制及不同模式之间的很强的整体相关行为。HT-6B上的实验结果表明,RHF对锯齿振荡过程也有显著的影响。近来的实验结果显示,RHF对MHD模式及锯齿振荡的作用过程中伴随着等离子体约束的改善。这一结果使得RHF影响等离子体行为的基本图像变得更加复杂。

## 二、在RHF作用下的锯齿振荡

在比较宽的运行参数范围内,即 $\bar{n}_e = (0.6 \sim 3) \times 10^{13} \text{cm}^{-3}$ 、 $q=2.5 \sim 5$ , HT-6B托卡马克上的锯齿振荡现象均受到RHF的影响。RHF的最佳幅值及最佳位形( $l=2$ 或 $l=3$ )取决于托卡马克运行条件。不过RHF的强度不超过极向场的1%,下面给出根据等离子体密度大小划分的两个运行区中的实验结果。

第一个运行区为低密度( $\bar{n}_e < 1.5 \times 10^{13} \text{cm}^{-3}$ )。在这个运行区内,通常放电中的锯齿振荡被RHF放大。图1(a)(见5页)给出了由软X射线二极管阵列探测到的信号及 $m=1$ 的磁扰动信号随时间的发展。为了便于比较,图1(b)中给出了被RHF放大的锯齿振荡和在一次放电中RHF没有开启时的锯齿振荡。

在RHF于12ms处开启之后,锯齿振荡的幅度、周期和变化斜率均被放大。锯齿幅度约增加2.5%,此时锯齿振荡引起的扰动幅度大约是中心道软X射线测量信号的平均值的三分之一;锯齿周期由230 $\mu\text{s}$ 增加到320 $\mu\text{s}$ ;锯齿上升率由0.9V/ms增加到1.5V/ms;锯齿破裂斜率由3.6V/ms增加到7.9V/ms。

第二个运行区为密度较高区( $\bar{n}_e < 1.5 \times 10^{13} \text{cm}^{-3}$ )。在该运行区内,放电过程中通常有很强Mirnov振荡,磁扰动的幅值大约是极向场的1%。在图2(a)中,软X射线信号和Mirnov探针信号被频率为24kHz的扰动所调制。在8ms时开启RHF后,Mirnov振荡转变为锯齿振荡,其幅度比图1中给出的锯齿振荡的幅度还要大。在某些放电中,RHF还能使锯齿振荡在小半径 $r=10\text{cm}$ 处的软X射线信号(限制器半径为12.5cm)和Mirnov探针信号上出现。

图2(b)和图2(c)(见6页)分别给出了RHF开启和关断两个时刻附近的软X射线信号随时间的发展。可以看出,当RHF开启时,频率为24kHz的扰动幅度减小,而具有较大的幅度的锯齿振荡在整个等离子体小截面上均出现;在RHF关断时,发生了相反的过程。这两个转变过程的时间尺度均在1ms左右,非常接近HT-6B托卡马克的能量约束时间 $\tau_E \sim 0.7\text{ms}$ 。

在两个运行区中, $m=1$ 的扰动出现在 $r < 4\text{cm}$ 的区域,而 $m=2,3$ 的扰动则出现在 $r > 8\text{cm}$ 的区域,RHF使扰动模式的抑制和锯齿振荡的出现同时发生。这对锯齿破裂的驱动力问题提供了一个论据,即被抑制了的很小的 $m=1$ 扰动不可能在等离子体热心驱动那样强的锯齿破裂。

### 三、RHF改善等离子体的约束

根据不同小半径处的锯齿振荡之间的时间延迟可以推算出电子热导系数<sup>[4]</sup>。表1(见4页)给出了HT-6B托卡马克上的结果。可以看出, RHF使得等离子体中心区和边缘区的电子热导系数分别减小到 $3/4$ 和 $2/3$ 。电子热导的减小与前面所述的锯齿上升率的增加很好地一致。

由软X射线辐射测量获得的电子温度分布在图3(见7页)中给出。可以看出, RHF使得电子温度分布变“胖”, 外部区域内( $r > r_s$ )  $T_e$ 增加而中心区 $\bar{T}_e$ (对锯齿振荡平均)有较明显的减小。等离子体中心区电子温度的减小可能与放大的锯齿振荡有关, 因为大的锯齿振荡使得 $T_e$ 能达到一个较大的最大值的时, 也能在锯齿破裂时使 $T_e$ 达到一个更小的最小值。在我们的实验中, 还观察到等离子体的线平均密度 $\bar{n}_e$ 在RHF作用下随着时间的推移而渐渐增加。例如, 在相同的补充充气条件下, 连续两次实验参数相同的放电中, 不加RHF的放电的密度 $\bar{n}_e = 1.1 \times 10^{13} \text{cm}^{-3}$ , 而在加了RHF的放电中,  $\bar{n}_e$ 可达 $1.6 \times 10^{13} \text{cm}^{-3}$ 。

图4(见7页)给出了RHF实验中光谱线辐射的测量结果。OIII线(375.89nm) CIII线(464.74nm)和H $\alpha$ 线(656.3nm)由具有0.6cm空间分辨的多通道光纤输出的单色仪监测。可以看出, 轻杂质的线辐射在8ms到14.2ms的RHF开启时间内出现一个平台, 其幅值大约是初始值的一半; 其上升和下降过程分别与图2(b)和图2(c)中的锯齿振荡的转变过程相对应。这种平台现象在从中心到边缘(11cm处)的所有观察弦的光谱信号上都出现。就现有的实验数据来说这一现象还不易解释。平台的上升时间和下降时间均为1ms, 显然杂质的新经典累积和扩散都没有这么快, 因此需要进一步进行精密的诊断和仔细的理论计算。

在图4中还可以看出, H $\alpha$ 线辐射与杂质辐射有所不同, 即在加RHF后2ms的时间内H $\alpha$ 线辐射增加, 然后又衰减到原来的水平。并且, 当RHF关断时, H $\alpha$ 线辐射没有明显的变化, 这说明在加有RHF期间没有很强的氢通量进入等离子体。

综上所述, 弱的RHF能改变MHD不稳定性、锯齿振荡行为以及等离子体的约束。另一方面RHF的上述作用依赖于等离子体的条件。一般在高 $Z_{\text{eff}}$ 时, RHF没有明显的作用。不同的RHF波形( $l=2$ 或 $l=3$ )也必须与不同的 $q$ 值和分布相匹配, 才能对等离子体有明显的作用。而且RHF的最佳强度与等离子体密度有关。这些意味着不能把RHF对等离子体的作用简单地认为是RHF与MHD不稳定性模式之间的直接相互作用。

### 四、结 论

主要的实验结果归纳如下:

(a) RHF能减少能量和粒子损失从而改善等离子体的约束。有RHF的放电具有较高的等离子体密度和较“胖”的温度分布;

(b) RHF加大锯齿振荡表现在使锯齿振荡幅度增加、周期变大、斜率增加及使锯齿振荡出现在更大的空间区域内。具有很强的锯齿破裂的锯齿振荡使等离子体中心区的平均电子温度下降。至于是什么样的驱动力导致锯齿破裂以及驱动力被加强还不清楚。

(c) 在加有RHF时, 等离子体整个空间范围内的轻杂质辐射增加并呈现出一个平台。

这与等离子体密度的连续增加不同。

(d) 一个直流RF不仅能抑制Mirnov振荡，改善等离子体的约束，而且能放大锯齿振荡、增强杂质辐射等等。从通常托卡马克放电的物理图像很难理解这一现象。它似乎是托卡马克等离子体处于一个新的状态。

# CHINA NUCLEAR SCIENCE & TECHNOLOGY REPORT



P.O.Box 2103

书号: 15175-00304

Beijing, China

## China Nuclear Information Centre

---